Cooperative DNA Binding by the B-Isoform of Human Progesterone Receptor: Thermodynamic Analysis Reveals Strongly Favorable and Unfavorable Contributions to Assembly†

Aaron F. Heneghan, Keith D. Connaghan-Jones, Michael T. Miura, and David L. Bain*

Department of Pharmaceutical Sciences, University of Colorado Health Sciences Center, 4200 East 9th Avenue, Denver, Colorado 80262

Received October 7, 2005; Revised Manuscript Received January 10, 2006

ABSTRACT: Progesterone receptors (PR) play critical roles in eukaryotic gene regulation, yet the mechanisms by which they assemble at multisite promoters are poorly understood. Here we present a thermodynamic analysis of the interactions of the PR B-isoform (PR-B) with promoters containing either one or two progesterone response elements (PREs). Utilizing quantitative footprinting, we have resolved the microscopic energetics of PR-B binding, including cooperativity terms. The results of this analysis challenge a number of assumptions found in traditional models of receptor function. First, PR-B interactions at a single PRE can be equally well described by mechanisms invoking either the receptor monomer or the dimer as the active DNA binding species. If, as is commonly accepted, PR-B interacts with response elements only as a preformed dimer, then its intrinsic binding affinity is not the typically observed nanomolar but is rather picomolar. This high affinity binding is opposed, however, by a large energetic penalty. The penalty presumably pays for costly structural rearrangements of the receptor dimer and/or response element that are needed to form the protein−DNA complex. If PR-B assembles at a single response element via successive monomer binding reactions, then this penalty minimizes cooperative interactions between adjacent monomers. When binding to two response elements, the receptor exhibits strong intersite cooperativity. Although this phenomenon has been observed before, the present work demonstrates that the energetics reach levels seen in highly cooperative systems such as λ *c*I repressor. This first quantitative dissection of cooperative receptor−promoter interactions suggests that PR-B function is more complex than traditionally envisioned.

Progesterone receptors (PR)[1] are members of the nuclear receptor superfamily of ligand-regulated transcription factors (*1*). An understanding of PR function is complicated by the fact that the receptor exists as two naturally occurring isoforms: an 83 kDa A-receptor (PR-A) and a 99 kDa B-receptor (PR-B). The two proteins are identical except for a 164-amino-acid extension at the N-terminus of PR-B (see Figure 1). Both isoforms are characterized by a centrally located DNA binding domain (DBD) and a C-terminal hormone binding domain (HBD). The two domains are linked by a 50-amino-acid "hinge" sequence of unclear function. Transcriptional activation functions are located N-terminal to the DBD (AF-1) and within the HBD (AF-2). The 164 residues unique to PR-B contain a context-dependent transcriptional activation function (AF-3) (*2*).

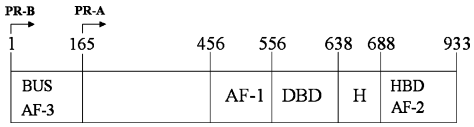

FIGURE 1: Progesterone receptor domain structure. Schematic of primary amino acid sequence for PR-A and PR-B isoforms. Functional regions are as indicated: DBD, DNA binding domain; HBD, hormone binding domain; H, hinge; AF, activation function; BUS, B-unique sequence. PR-B is defined as amino acids 1−933, PR-A is defined as amino acids 165−933.

Despite their high degree of sequence identity, the two isoforms have distinctly different functional properties. For example, the B-isoform is typically a much stronger transcriptional activator than the A-isoform (*3*), the two receptors regulate different subsets of genes (*4*), the isoforms respond differently to progestin antagonists such as RU486 (*5*), and they play different roles in target tissues such as the breast and uterus (*6*). At the clinical level, recent work has demonstrated that breast cancer patients with an excess of PR-A have a poorer prognosis compared to patients with an excess of PR-B (*7*). We are interested in the origins of these isoform-specific functional differences, and in particular, the quantitative principles by which the isoforms assemble at complex promoters and activate transcription.

Progesterone receptors are affiliated with the steroid receptor family, a subdivision of the nuclear receptor

† This work was supported by NIH Grants R01-DK061933 to D.L.B. and F32-DK070519 to A.F.H., and the Tissue Culture Core Laboratory of the UCHSC Cancer Center.

* To whom correspondence should be addressed: Department of Pharmaceutical Sciences, C-238, University of Colorado Health Sciences Center, 4200 E. 9th Ave, Denver, CO 80262. Phone: 303-315-1416. Fax: 303-315-0274. E-mail: David.Bain@UCHSC.edu.

[1] Abbreviations: PR, progesterone receptor; PR-A, progesterone receptor A-isoform; PR-B, progesterone receptor B-isoform; PRE, progesterone response element; DBD, DNA binding domain; HBD, hormone binding domain; BUS, B-unique sequence; AF, activation function; MMTV, mouse mammary tumor virus.

10.1021/bi052046g CCC: $33.50
Published on Web 02/16/2006

superfamily. Other steroid receptor family members include the estrogen receptor, glucocorticoid receptor, mineralocorticoid receptor, and androgen receptor. Traditional models of steroid receptor function propose that upon binding their cognate hormone, the receptors dimerize, translocate to the nucleus, bind to their DNA response elements at upstream promoter sites, and recruit an array of coactivating proteins to activate transcription (*1*). In the case of PR (defined here as a composite of both isoforms), evidence in support of the early steps of this pathway was based on immuno-isolation, chemical cross-linking, and gel-shift studies that demonstrated partially purified receptor was capable of dimerizing in solution and that only the dimer appeared competent to bind to palindromic progesterone response elements (PREs), typically with apparent nanomolar affinity (*8*−*10*). Studies of the other steroid receptor family members suggested that the hormone binding domain was the primary mediator of solution dimerization. Additionally, the monomeric DNA binding domain of steroid receptors was shown to dimerize upon binding a single palindromic response element, indicative of "intrasite" cooperativity (*11*).

In parallel with these biochemical studies, transient transfection assays demonstrated that PR could only weakly activate transcription of a reporter gene when the promoter contained a single palindromic PRE (*12*). In contrast, when a pair of tandemly linked palindromic PREs (PRE_2) was placed upstream of the reporter gene, PR could strongly activate transcription, indicative of transcriptional synergy. Gel shift analysis of the interactions of PR with DNA fragments containing the above palindromic response elements demonstrated that PR exhibited "intersite" cooperativity, causing a 100-fold enhancement of overall binding affinity on the synthetic PRE_2 DNA fragment compared to a fragment containing a single PRE (*12*). Thus, the synergistic increase in transcriptional activity seen with tandemly linked response elements was interpreted to be due to cooperative interactions between adjacently bound PR dimers.

Reactions in which protein self-assembly in solution (e.g., dimerization) is coupled to cooperative, high-affinity DNA binding appear to be a common first step in regulating transcriptional activation. However, it is not clear whether this type of mechanism is sufficient to explain all aspects of progesterone receptor (and perhaps steroid receptor) transcriptional function. For example, natural PR-regulated promoters tend not to exhibit clearly recognizable symmetric and palindromic binding sites that would be targets for ligand-activated PR dimers (*13*). Instead, computer analysis suggests that natural PR recognition sequences are made up of clustered half-sites that may or may not have an adjacent, and only moderately conserved, half-site (B. M. Jacobsen and K. B. Horwitz, personal communication). Moreover, qualitative footprinting studies of PR interactions with natural promoters containing multiple response elements showed little evidence of cooperative binding (*14*), even though mutational analysis of the binding sites revealed synergistic transcriptional activation properties (*15*). Finally, it is not entirely clear that progesterone receptors bind to palindromic response elements only as preformed dimers. Although there appears to be no evidence that full-length receptor monomers can bind to isolated half-sites (*13*), early biochemical studies indicated that the closely related glucocorticoid receptor could bind to clustered half-sites possibly as a monomer (*16*) or possibly as a dimer (*17*). Keeping in mind that these pioneering studies were necessarily carried out using partially purified receptor preparations and semiquantitative techniques, it seems reasonable to state that the definitive analysis of the pathway(s) by which receptors bind to response elements has yet to be carried out.

As a first step toward obtaining a quantitative understanding of PR function, we have carried out a thermodynamic analysis of the interactions of full-length, human PR-B with promoters containing either one or two palindromic PREs. Through a global analysis of all datasets, we have resolved the microscopic free energy contributions to binding, including intersite and intrasite cooperativity terms. This study thus represents the first energetic dissection of a cooperative protein−DNA binding reaction using an intact nuclear receptor and a multisite promoter. Moreover, the results demonstrate that cooperative PR-B binding affinity is not only dramatically greater than previously assumed but that binding is heavily penalized, presumably due to structural alterations in the protein and/or DNA. Large, opposing contributions to binding have been observed in other DNA binding proteins and may serve here as a means to efficiently control PR-regulated gene expression.

MATERIALS AND METHODS

Expression and Purification of the Full-Length B-Isoform of Human Progesterone Receptor. An expression vector encoding residues 1−933 of PR-B fused to an N-terminal hexahistidine sequence was a generous gift of Dr. Dean Edwards (University of Colorado Health Sciences Center). PR-B was expressed in baculovirus-infected Sf9 insect cells as previously described (*18*). A detailed description of the PR-B purification and a quantitative analysis of its solution properties were also previously described (*19*). To summarize, 95% pure PR-B is highly active in hormone binding activity, quantitatively exists as an equilibrium distribution of monomers and dimers as judged by analytical ultracentrifugation, and has a dimerization free energy (ΔG_{di}) of −7.2 kcal/mol under conditions identical to those used in the present analysis. Since accurate estimates of DNA binding energetics require an independently determined solution dimerization free energy, ΔG_{di} was held as a constant during analysis of the footprint titration data. Finally, the DNA binding activity of the receptor was assumed to be 100%.

DNA Preparation for DNase I Footprinting. A vector containing a synthetic PRE_2 promoter template was a generous gift of Dr. Kathryn Horwitz (University of Colorado Health Sciences Center). This promoter contains two tandemly linked PREs, each corresponding to the palindromic tyrosine aminotransferase promoter sequence (TGTACAGGATGTTCT) (*20*). The PREs are spaced 25 bp apart and upstream of a thymidine kinase regulatory element. Generated "in house" was a reduced-valency promoter template (PRE_{1-}) containing a G-to-T point mutation in each half-site of the distal PRE (designated as site 1), thus eliminating PR-B binding to that palindrome (*21*). The templates were excised from their respective vectors with a *Nae* I and *Hind* III digestion, resulting in 1304-bp fragments. The fragments were purified and ^{32}P-end-labeled on the sense-strand using a Klenow fill-in reaction (*22*). The proximal PRE of each fragment was positioned 100 bp from the 3′ end of the labeled strand.

Table 1: Species Distributions, Free Energy Changes, and Interaction Constants for Monomer and Dimer Assembly Pathways for PR-B

	Monomer Pathway			Dimer Pathway		
Representative Species Diagram[1]	Number of configurations[2]	Microscopic Constant	Free Energy Contribution[3]	Number of Configurations[2]	Microscopic Constant	Free Energy Contribution[3]
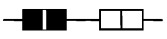	1	-	reference state	1	-	reference state
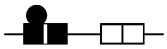	4	k_1	ΔG_1	-	-	-
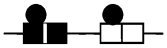	4	k_1^2	$2{\cdot}\Delta G_1$	-	-	-
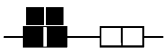	2	$k_1^2{\cdot}k_{c1}$	$2{\cdot}\Delta G_1 + \Delta G_{c1}$	2	$k_{di}{\cdot}k_2$	$\Delta G_{di} + \Delta G_2$
	4	$k_1^3{\cdot}k_{c1}$	$3{\cdot}\Delta G_1 + \Delta G_{c1}$	-	-	-
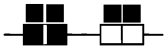	1	$k_1^4{\cdot}k_{c1}^2{\cdot}k_{c2}$	$4{\cdot}\Delta G_1 + 2{\cdot}\Delta G_{c1} + \Delta G_{c2}$	1	$k_{di}^2{\cdot}k_2^2{\cdot}k_{c2}$	$2{\cdot}\Delta G_{di} + 2{\cdot}\Delta G_2 + \Delta G_{c2}$

[1] Each diagram represents one of the possible microscopic configurations at each ligation state. [2] Number of possible configurations at ligation state. [3] Each free energy change is related to each microscopic association constant through the standard relationship $\Delta G_i = -RT \ln k_i$, where R is the gas constant and T is the temperature in Kelvin.

Individual-Site Binding Experiments. Experiments were carried out using quantitative DNase I footprint titrations as originally described by Ackers and co-workers (*23*, *24*), with the following modifications. All reactions were carried out in an assay buffer containing 20 mM Hepes, pH 8.0, 50 mM NaCl, 1 mM DTT, 1 mM $CaCl_2$, 2.5 mM $MgCl_2$, 1×10^{-5} M progesterone, 100 μg/mL BSA, and 2 μg/mL salmon sperm DNA. Each reaction contained 20 000 cpm of freshly labeled DNA containing either the PRE_2 promoter or PRE_{1-} promoter. PR-B was added to each reaction mix, covering a concentration range from sub-nanomolar to micromolar, and the sample was allowed to equilibrate at 4 °C for at least 45 min. DNase I (Invitrogen) was diluted to a concentration of 0.0058 units/μL in the assay buffer less BSA and salmon sperm DNA. After the samples reached equilibrium, 5 μL of the diluted DNAse I solution was added to each 200 μL reaction, and digestion was allowed to proceed for exactly 2 min. Digestion products were electrophoresed on 6% acrylamide-urea gels and visualized using phosphorimaging. Individual-site binding isotherms were calculated as described by Brenowitz et al. (*23*) using the program, ImageQuant.

The thermodynamic validity of the quantitative DNase footprint titration technique is based upon the testable assumptions that the system of interest is at equilibrium and that DNase exposure does not perturb that equilibrium (*23*). In the present study, the resolved binding isotherms were independent of equilibration times from 45 min to 2 h. Control experiments that varied DNase activity but kept enzymatic exposure time constant generated identical results. Control experiments that varied DNase exposure time but kept total DNase activity constant (e.g., halving the DNAse concentration but doubling exposure time) also generated identical results, thus demonstrating that the results were not confounded by kinetic artifacts. All studies presented here were carried out with DNase concentrations that approximated "single hit kinetics" (*23*). Finally, promoter DNA concentrations were estimated to be well below PR-B binding affinity (maximally 5 pM), thus justifying the assumption that $PR\text{-}B_{free} \sim PR\text{-}B_{total}$.

Resolution of Microscopic Interaction Free Energies. The interactions of PR-B at the PRE_2 promoter were described using the following model, composed of the pathways represented in Figure 2a,b. The ligation state configurations and species distributions accessible in this model are shown in Table 1, as are the corresponding equilibrium constants and free energy contributions necessary to construct the mathematical expressions for PRE binding. The model makes the following assumptions: (1) PR-B exists under the stated solution conditions as a monomer−dimer equilibrium. This "assumption" can be taken as fact in light of our previous work on the energetics of PR-B solution self-assembly (*19*). (2) PR-B can follow either a monomer pathway (Figure 2b) or preformed dimer pathway (Figure 2a) to DNA binding; monomers can bind to individual half-sites (ΔG_1) and dimers can bind to palindromic sites (ΔG_2). The validity of this assumption is based on biochemical studies demonstrating that preformed PR dimers bind to response elements (*9*) but that solution dimerization may not always be prerequisite to PRE binding and transcriptional activation (*25*−*27*). (3) Monomers bind with identical affinity (ΔG_1) to each half-site within the palindromic tyrosine aminotransferase PRE. This assumption was validated based on our initial analysis of PR-B binding to the PRE_{1-} promoter; see Results section. (4) A monomer bound to a PRE half-site can cooperatively recruit another monomer to the half-site within a palindromic PRE but not between palindromic PREs (thus defining "intrasite" cooperativity, ΔG_{c1}). Evidence in support of this assumption comes from biophysical studies that demonstrated that monomeric DBDs of GR and monomeric N-terminal constructs of PR bind cooperatively to half-sites separated by three base pairs (i.e., palindromic response element) (*17*, *25*, *26*); however, half-sites separated by more than 15 base pairs could not mediate cooperative GR or PR interactions (*14*, *17*). (5) Cooperativity between palindromic PREs (defined here as "intersite" cooperativity, ΔG_{c2}) only occurs when all PREs are fully ligated, either by four monomers or two dimers. This assumption is based upon previous semi-quantitative analyses of cooperative PR−PRE interactions indicating that PR dimers bind cooperatively to multisite promoters (*12*).

The DNase I footprint titration technique resolves the fractional occupancy of binding at each PRE. The statistical thermodynamic expressions that describe the individual-site binding isotherms are constructed by summing the probabilities of each microscopic species that contributes to

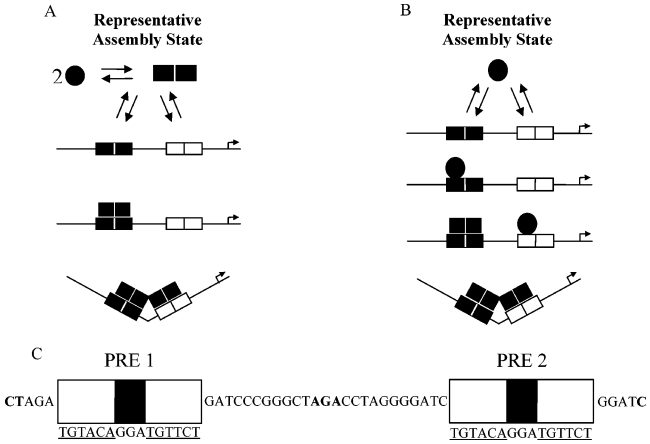

FIGURE 2: Schematic representation of selected assembly states for PR-B:PRE_2 interactions. (A) Dimer binding pathway: Filled circles represent hormone-bound PR-B structure prior to either solution dimerization or cooperative binding at a PRE. Filled squares represent PR-B solution dimers or PR-B bound to the PRE_2 promoter template. Only preformed PR-B dimers are competent to assemble at palindromic response elements. Binding at multiple response elements is accompanied by cooperative interactions between the sites (defined here as "intersite cooperativity") seen as direct contact of adjacently bound dimers and induction of DNA bending. (B) Monomer binding pathway: PR-B assembles at palindromic response elements via a succession of monomer-binding reactions. Successive binding at an individual response element is accompanied by cooperative interactions (defined here as "intrasite cooperativity") and represented by a transition from a filled circle to a filled square. In both panels, PRE binding sites within the PRE_2 template are represented by a solid rectangle (site 1) and open rectangle (site 2). Separating each half-site within each PRE is a white line (site 1) or a black line (site 2). Arrow refers to the direction of transcriptional start site. (C) Nucleotide sequence of the PRE_2 promoter in the vicinity of the two PREs. Underlined sequences correspond to half-sites of each palindromic response element. Nucleotides in bold correspond to the approximate locations of hypersensitive bands appearing in the Quantitative Footprint Titrations; see Results for details.

binding at that site. A detailed approach for constructing each mathematical formulation has been presented previously (*28*). Briefly, the probability (f_s) of each microscopic species is defined as (*29*):

$$f_S = \frac{e^{(-\Delta G_S/RT)}[x]^j}{\sum_{S=1}^{j} e^{(-\Delta G_S/RT)}[x]^j} \quad (1)$$

where ΔG_s is the free energy of configuration *s* relative to the unliganded reference state, *x* is the PR-B monomer concentration (calculated from the dimerization constant, k_{di}), and *j* is the stoichiometry of PR-B monomer bound to a response element. *R* is the gas constant, and *T* is temperature in Kelvin. The relationship between each free energy change and its association constant is defined via the standard relationship $\Delta G_i = -RT \ln k_i$. Thus, the fractional saturation ($\bar{Y}$) for dimer binding at site 1 of the PRE_2 promoter is the sum of probabilities for the isolated dimer binding reaction and the cooperative binding reaction with the adjacently bound dimer. When expressed in units of free monomer concentration, the fractional saturation is then defined as

$$\bar{Y}_{PRE_2} = \frac{k_{di}k_2x^2 + k_{di}^2k_2^2k_{c2}x^4}{1 + 2k_{di}k_2x^2 + k_{di}^2k_2^2k_{c2}x^4} \quad (2)$$

where k_{di} and *x* are as defined above, k_2 is the intrinsic association affinity for dimer binding to a palindromic site, and k_{c2} corresponds to the intersite cooperativity term. The association equilibrium constants are presented in lower-case to emphasize that they represent microscopic interactions rather than traditional (upper-case) macroscopic interactions. Finally, because the palindromic PREs in the PRE_2 promoter are identical in sequence, the above equation also describes binding at site 2 in the context of the PRE_2 promoter.

The fractional saturation for binding at site 2 of the PRE_{1-} promoter (i.e., binding to an isolated PRE) via a dimer pathway when expressed in units of free monomer concentration is then

$$\bar{Y}_{PRE_{1-}} = \frac{k_{di}k_2x^2}{1 + k_{di}k_2x^2} \quad (3)$$

Using the same approach to describe binding via a monomer pathway, the expressions for binding at each palindromic PRE within the PRE_2 promoter and at the palindromic PRE of the PRE_{1-} promoter are expressed as eqs 4 and 5, respectively:

$$\bar{Y}_{PRE_2} = \frac{2k_1x + 4k_1^2x^2 + k_1^2k_{c1}x^2 + 4k_1^3k_{c1}x^3 + k_1^4k_{c1}^2k_{c2}x^4}{1 + 4k_1x + 4k_1^2x^2 + 2k_1^2k_{c1}x^2 + 4k_1^3k_{c1}x^3 + k_1^4k_{c1}^2k_{c2}x^4} \quad (4)$$

$$\bar{Y}_{PRE_{1-}} = \frac{2k_1x + k_1^2k_{c1}x^2}{1 + 2k_1x + k_1^2k_{c1}x^2} \quad (5)$$

where k_1 refers to the intrinsic affinity of monomer binding, k_{c1} corresponds to the intrasite cooperativity, and *x* and k_{c2} are as defined previously. To resolve the above microscopic equilibrium constants, the two binding isotherms generated from the PRE_2 template and the single binding isotherm from the PRE_{1-} template were analyzed simultaneously using the program, Scientist (Micromath, Inc.). Because protein interactions at specific DNA binding sites do not afford complete protection from DNAse activity, binding data were treated as transition curves fitted to upper (*m*) and lower (*b*) endpoints using the equation:

$$\bar{Y}_{app} = b + (m - b)\bar{Y} \quad (6)$$

Finally, the independently determined equilibrium constant for solution dimerization was fixed at 4.7×10^5 M^{-1} for all analyses.

RESULTS

The commonly accepted kinetic pathway describing PR−PRE interactions is that hormone-bound receptor dimerizes in solution and then binds at its cognate response elements. For promoters containing two tandemly linked response elements, dimer binding is also coupled to cooperative

interactions between each site. This series of reactions is described schematically in Figure 2a; the quantitative distribution of the predicted microstates and the microscopic energetics are shown in Table 1. In light of our previous work demonstrating that PR dimerizes in solution only weakly (*19*), with a dimerization constant in the micromolar range when apparent DNA binding affinity is in the nanomolar range, we also describe a thermodynamically equivalent, alternative pathway by which PR monomers bind at each half-site, cooperatively recruit another PR monomer, and generate intersite cooperativity as seen in the dimer pathway. This mechanism is shown as the reaction in Figure 2b and in Table 1. Quantitative DNase I footprint titrations of promoters containing either one or two palindromic response elements were used to resolve the microscopic energetics associated with each pathway. The specific binding site sequences and DNA sequence surrounding the two palindromic response elements are shown in Figure 2c.

Shown in Figure 3a is a quantitative footprint titration of the PRE_{1-} promoter template. It is evident that PR-B binding is specific for the intact PRE (site 2) over a broad range of protein concentrations. (Dideoxy sequencing analysis indicates that the DNAse protected region included the entire palindromic PRE and one to two additional nucleotides on either side of the PRE). By contrast, point mutations in each half-site of site 1 eliminate PR-B binding to that sequence. Coincident with PR-B binding is the appearance of hypersensitive sites directly adjacent to the boundaries of site 2. As highlighted in Figure 2c, these sites mostly likely correspond to nucleotides located four to five basepairs outside the canonical PRE. This increased nicking of the DNA does not reflect an artifact of PR-B influence on DNase activity (*30*) since the effect was independent of the amount or type of carrier DNA present (data not shown). Protein-induced hypersensitivity is typically attributed to DNA bending. Consistent with this, circular permutation analysis of PR−PRE interactions demonstrated that both PR isoforms bent DNA when interacting at individual response elements (*31*).

Shown in Figure 3b is the binding isotherm generated from integration of band intensities for five independent PRE_{1-} footprint titration experiments. When plotted in units of total PR-B concentration, it is evident that half-saturation of the PRE site occurs at approximately 12 nM PR-B. When the binding data are fit to a phenomenological Hill equation, $\bar{Y} = kx^n/(1 + kx^n)$, we resolve an n of 1.5 ± 0.2, indicative of a moderate cooperative effect consistent with the shallow transition of the binding isotherm. Since the binding data are presented in units of total protein concentration, the origin of this effect must be due to cooperativity arising from a linked PR-B solution dimerization reaction, or DNA-induced cooperative dimerization of PR-B monomers.

Presented in Figure 4a is the footprint of the PRE_2 promoter template. As seen with the PRE_{1-} template, receptor binding is site-specific, with protection corresponding to the entire response elements and one to two neighboring basepairs. Binding is again accompanied by the appearance of weak hypersensitive sites (small arrows) four to five basepairs from each response element. However, seen only on the PRE_2 template is a more intense hypersensitivity induced in the region between response elements (large arrow). Since we show below that receptor binding to the

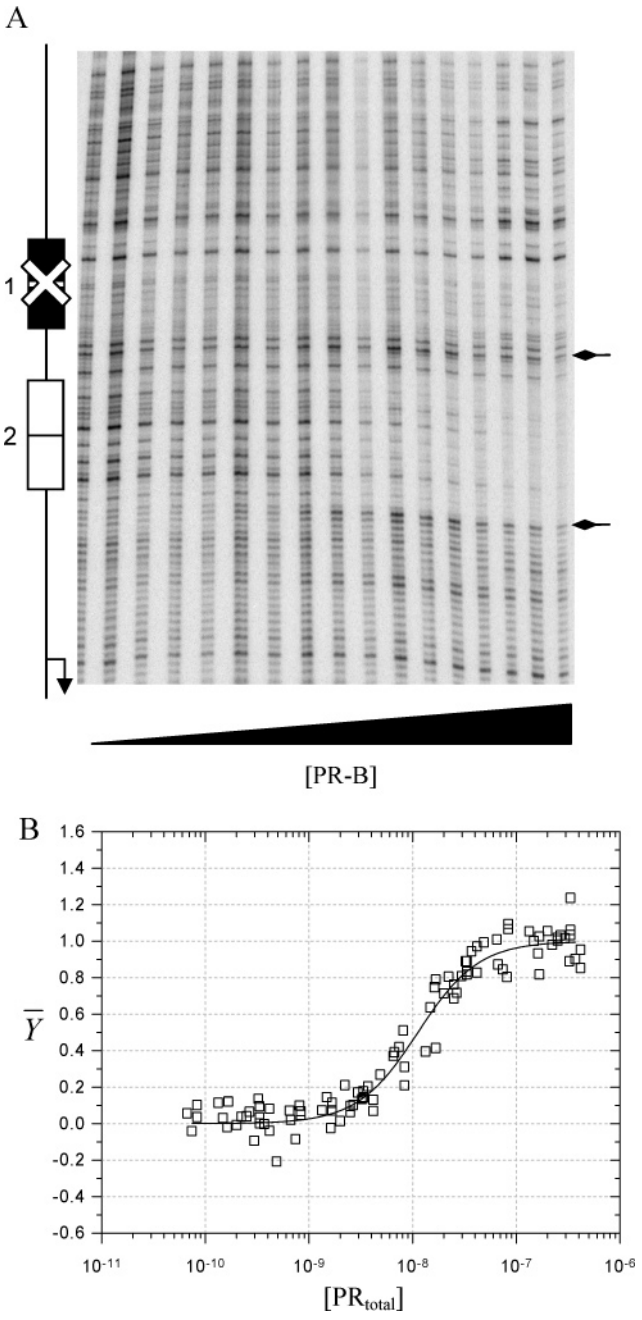

FIGURE 3: Representative quantitative footprint titration and individual-site binding isotherms obtained for PR-B binding to the PRE_{1-} promoter. (A) PRE_{1-} footprint titration image. Schematic of PRE_{1-} promoter structure is shown to left. PRE site 1 is indicated by the filled rectangle with a white line separating each half-site. Binding at site 1 in the PRE_{1-} has been eliminated as indicated by the "X". PRE site 2 is indicated by the open rectangle, with a black line separating each half-site. The downward arrow indicates the direction of transcriptional initiation start site. Diamond headed arrows (right of image) indicate the appearance of hypersensitive bands seen on both the PRE_{1-} and PRE_2 promoter templates. PRE sites were determined by dideoxy sequencing. (B) Binding isotherm generated from five independent footprint titration experiments. Open squares represent binding at site 2 of the PRE_{1-} promoter. The line through the data represents best-fit analysis of all datasets to the Hill equation.

PRE_2 promoter is coupled to intersite cooperative interactions, the appearance of this second type of hypersensitivity suggests that cooperativity between PREs is accompanied by additional bending or deformation of the promoter

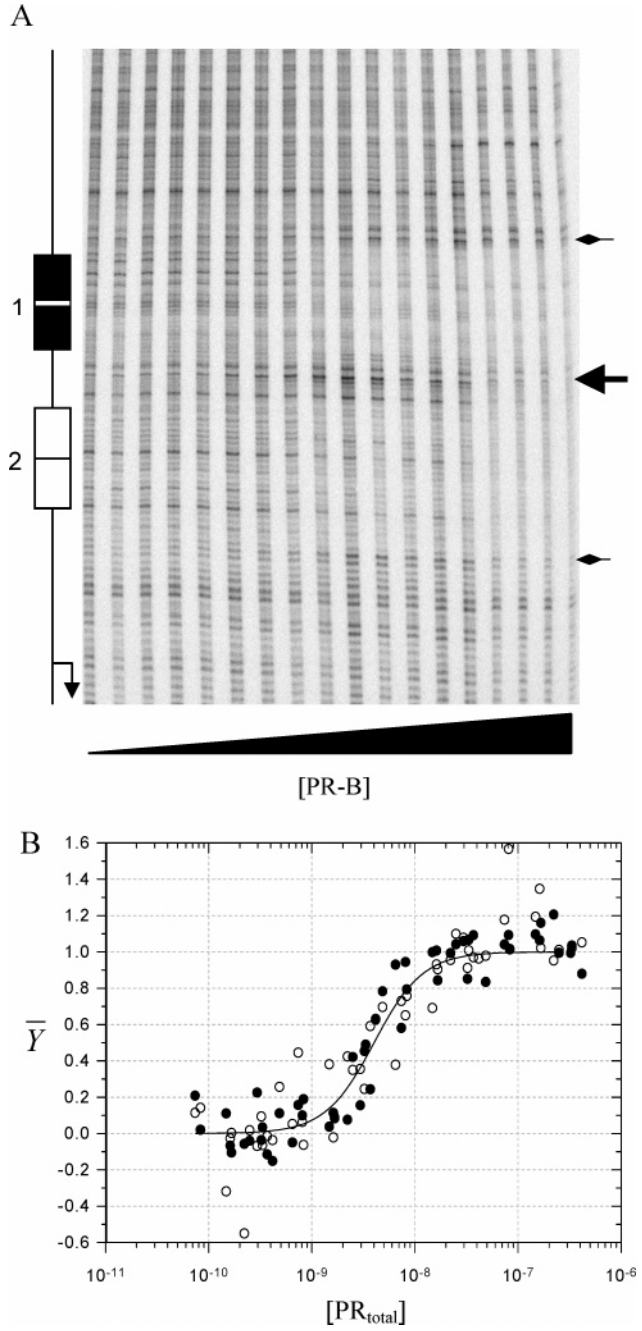

FIGURE 4: Representative quantitative footprint titration and individual-site binding isotherms obtained for PR-B binding to the PRE_2 promoter. (A) PRE_2 footprint titration image. Schematic of PRE_2 promoter structure is shown to left. PRE site 1 is indicated by the filled rectangle with a white line separating each half-site. PRE site 2 is indicated by the open rectangle, with a black line separating each half-site. The downward arrow indicates the transcriptional initiation start site. Diamond headed arrows (right of image) indicate the appearance of hypersensitive bands seen on both the PRE_{1-} and PRE_2 promoter templates. Large arrow indicates the appearance of the hypersensitive bands seen only on the PRE_2 promoter template. PRE sites were determined by dideoxy sequencing. (B) Binding isotherms generated from three independent footprint titration experiments. Symbols represent binding at site 1 of the PRE_2 promoter (filled circles) and binding at site 2 of the PRE_2 promoter (open circles). The line through the data represents best-fit analysis of all individual-site binding isotherms to the Hill equation.

complex. Sequencing analysis indicates that the hypersensitive regions correspond to several nucleotides centrally located between the two palindromic response elements (see Figure 2c). At the highest PR-B concentrations, nonspecific binding is observed, seen as a footprint appearing over all DNA bands. Binding data generated at these high protein concentrations were not used in any subsequent analysis.

The isotherms for binding at sites 1 and 2 of the PRE_2 template (carried out in triplicate) are shown in Figure 4b. Separate analysis of binding at sites 1 and 2 using the Hill equation was made difficult by the noise in the data. However, collective fitting of the six individual-site binding isotherms to the Hill equation resolves an n of 1.8 ± 0.4, suggestive of additional cooperative contributions (likely due to interactions between the two palindromic binding sites) compared to binding at the PRE_{1-} promoter template. Consistent with this, the binding transitions occur with half-saturation values of 4 nM and are steeper in appearance compared to binding on the PRE_{1-} template (Figure 3.)

Preformed Solution Dimers Bind at DNA Response Elements with Picomolar Affinities. The data presented in Figures 3 and 4 indicate that PR-B binds with roughly nanomolar apparent binding affinity and that binding both within and between palindromic response elements is somehow cooperatively driven. However, this information lends minimal insight into the mechanisms by which PR-B assembles at a promoter template. One approach to elucidating these mechanisms is to resolve the intrinsic and cooperative binding energetics that make up the macroscopic apparent binding affinity. As described in Materials and Methods and in Table 1, this approach entails constructing physically meaningful equations that describe binding at each site, then carrying out a global analysis of all datasets. Equation 2, describing a reaction in which preformed (and hormone-bound) dimers bind at sites 1 and 2 of the PRE_2 promoter, and eq 3, describing preformed dimers binding at the PRE_{1-} promoter, were used to simultaneously fit the three datasets shown in Figures 3b and 4b. This model is also presented schematically in Figure 2a. As represented by the solid lines in Figure 5a, it is evident that the solution dimer binding model well describes the data. (Note: Since binding at sites 1 and 2 of the PRE_2 promoter is described by the same equation (eq 2), the two predicted isotherms overlay each other and thus appear as one blue line in Figure 5a). The resolved free energy values from the dimer pathway model are reported in Table 2. As shown, the intrinsic binding affinity of a liganded PR-B dimer toward an individual palindromic PRE (ΔG_2) is -12.8 kcal/mol, which translates to a dissociation constant of 81 pM. This strong intrinsic affinity contrasts with the nanomolar binding transitions seen in Figure 3 and typically observed in semiquantitative gel shift assays (*8*). The reason for this apparent paradox is that the PR-B dimerization dissociation constant under these solution conditions is only 2.1 μM (*19*). Thus, at a total PR-B concentration in the nanomolar range necessary to initiate DNA binding, the PR-B dimer concentration comprises less than 0.1% of the total protein population and is thus picomolar in concentration.

PR-B Binding to Multiple Response Elements Is Coupled to Significant Intersite Cooperativity. In the context of the preformed dimer binding model, the resolved intersite cooperative free energy (ΔG_{c2}) is -2.5 kcal/mol. This value translates into a 99-fold increase in overall stabilization of the fully ligated PRE_2 complex compared to a noncooperative

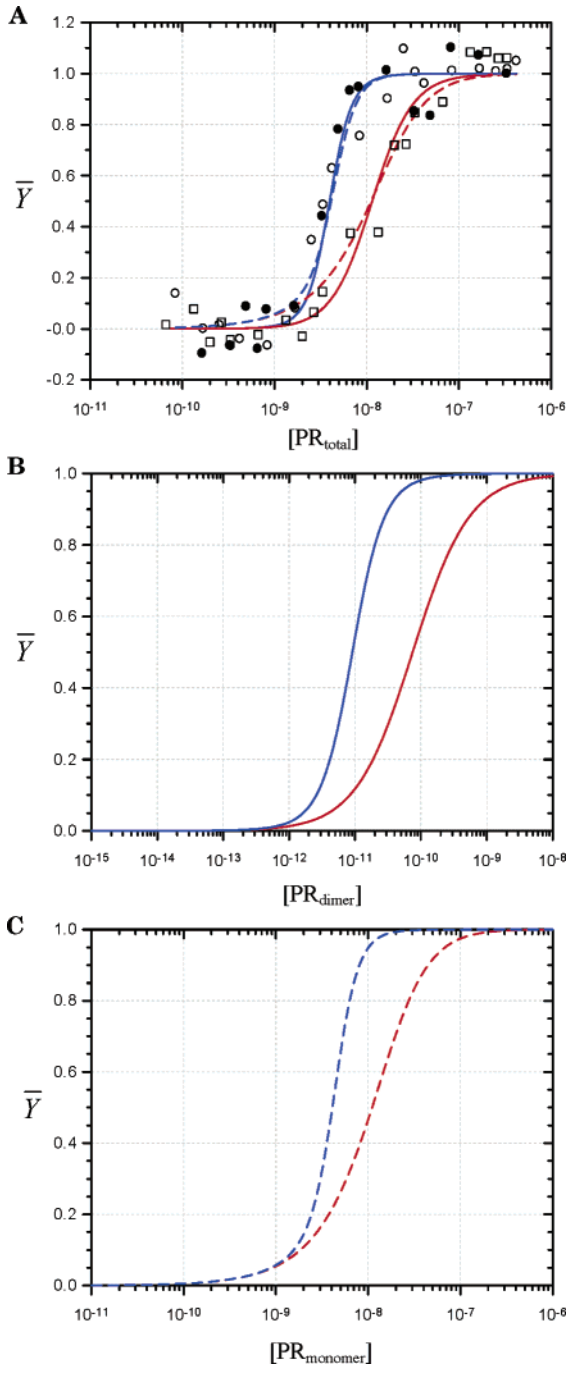

FIGURE 5: Pathway-dependent analysis of cooperative PR-B binding to the PRE_2 and PRE_{1-} promoters. (A) Individual-site binding isotherms and associated model dependent fits. Symbols represent binding at site 1 of the PRE_2 promoter (filled circles); binding at site 2 of the PRE_2 promoter (open circles); and binding at site 2 of the PRE_{1-} promoter (open squares). Lines represent best-fit global analysis of all data shown in Figures 3b and 4b using the dimer-binding pathway (solid lines; eqs 2 and 3) or monomer-binding pathway (dashed lines; eqs 4 and 5). For clarity, only a single representative set of footprint titrations are presented; all data seen in Figures 3b and 4b were used in the global analysis. Data are presented in units of total PR-B concentration. (B) Predicted binding isotherms from the best-fit dimer-binding pathway analysis presented in units of free PR-B dimer concentration (as calculated from the experimentally determined free energy of dimerization). Red and blue lines represent binding to PRE_{1-} and PRE_2 promoter templates, respectively. (C) Best-fit global analysis of the monomer-binding pathway presented in units of PR-B free monomer concentration. Red and blue lines represent binding to the PRE_{1-} and PRE_2 promoter templates, respectively.

Table 2: Resolved Free Energy Changes for PR-B/PRE_2 Binding Interactions[a]

monomer pathway[b] (kcal mol^{-1})	dimer pathway[c] (kcal mol^{-1})
$\Delta G_1 = -9.4 \pm 0.2$	$\Delta G_2 = -12.8 \pm 0.1$
$\Delta G_{c1} = -0.9 \pm 0.5$	$\Delta G_{c2} = -2.5 \pm 0.1$
$\Delta G_{c2} = -3.3 \pm 0.5$	$\Delta G_{di} = -7.2 \pm 0.74$

[a] Values calculated using $\Delta G_i = -RT \ln k_i$; errors correspond to 67% confidence intervals. [b] Square root of the variance was 0.071 apparent fractional saturation units. [c] Square root of the variance was 0.073 apparent fractional saturation units. [d] Free energy change for solution dimerization was measured independently using sedimentation equilibrium (*19*).

analogue. By basic theory (*32*), one can demonstrate that the 99-fold overall increase will partition to each PRE as the square root of the value, and thus appear as a nearly 10-fold increase in stabilization of binding for each site This degree of cooperativity is large enough to cause the binding isotherms to approach their asymptotic limits of steepness (*32*) and is comparable in value to that seen in classical interacting systems such as the λ repressor-right operator genetic switch (*28*). And yet, comparing the half-saturation values for binding at site 2 on the PRE_{1-} promoter (~12 nM) versus the PRE_2 promoter (~4 nM) there appears to be only a 3-fold per site enhancement of DNA binding affinity. The discrepancy once again occurs because the data are presented in units of total free PR-B concentration, rather than in units of the active binding species (i.e., PR-B solution dimer concentration). The discrepancy in apparent binding affinities and degree of cooperativity can be better appreciated in Figure 5b. Plotted are the binding isotherms for sites 1 and 2 of the PRE_2 promoter and site 2 of the PRE_{1-} promoter based on the resolved energetics, now presented in units of free PR-B solution dimer concentration (as calculated by the experimentally determined free energy of dimerization (*19*)). The 81 pM intrinsic binding affinity is now clearly revealed as a half-saturation value in the PRE_{1-} binding isotherm. Likewise, the 99-fold increase in overall binding affinity is more accurately visualized via the predicted approximate 10-fold increase in affinity at each site within the PRE_2 promoter compared to the PRE_{1-} promoter.

Energetics of a Putative Monomer Binding Pathway. Although it is clear that the data can be well described by a pathway in which only preformed, solution dimers bind DNA, our recent work demonstrating that hormone-bound PR-B is predominantly monomeric under the concentrations where DNA binding occurs (*19*) led us to evaluate the receptor monomer as the active DNA binding species. As noted in Materials and Methods, an assumption of this model is that the energetics of each putative monomer/half-site interaction are identical. The validity of this assumption is based on a detailed analysis of the PRE_{1-} binding data in isolation (See Figure 3). Quantitation of each half-site within the palindromic PRE (i.e., treating the palindromic site as two individual binding-sites) generated binding isotherms that, within error, were identical to each other and to the composite isotherm in Figure 3b. Identity of isotherm shape and affinity is suggestive but not conclusive evidence in favor of identical intrinsic affinities; if PR-B interactions at each half-site were of differing affinities but bound highly cooperatively, the curves would also appear to be nearly

identical. However, a highly cooperative binding reaction would be revealed by a steep binding transition—a type of transition not seen in the PRE_{1-} isotherm. Indeed, computer simulations suggest that the maximal amount of cooperative free energy and the maximal difference in the intrinsic half-site binding affinities that would still be consistent with the data are −1 and 0.35 kcal/mol, respectively (data not shown). These differences in the intrinsic binding affinities would be undetectable using quantitative footprinting. We thus conclude that putative monomer binding to each half-site is isoenergetic, at least within the noise of the data.

By globally fitting the three binding isotherms to a monomer pathway DNA binding model (Figure 2b and eqs 4 and 5), we resolved the intrinsic energetics of monomer binding to a PRE half-site (ΔG_1), an intrasite cooperativity term associated with recruiting a second monomer to the half-site (ΔG_{c1}), and an intersite cooperativity term defined as described previously for the preformed dimer binding model (ΔG_{c2}) (Tables 1 and 2). This analysis reveals several interesting results. First, as represented by the dashed lines in Figure 5a, the monomer binding model well describes the data. Second, the quality of the fit to the data is essentially identical to the dimer binding model (standard deviation of 0.071 apparent fractional saturation units for the monomer binding model versus 0.073 units for the dimer binding model). Put another way, the equilibrium binding data cannot distinguish between the alternative kinetic pathways represented in Figure 2. Third, the intrinsic energetics of a putative PR monomer binding reaction is −9.4 kcal/mol, which translates to a 39 nM dissociation constant. Finally, with regard to the intrasite cooperativity term, global analysis of the data resolved a value of only −0.9 kcal/mol. This weak interaction translates to only a 5-fold increase in binding affinity and is reflected in the shallow transition of the PRE_{1-} binding isotherm. The large error associated with this term arises because intrinsic binding affinities and cooperativity terms are typically highly correlated, making it difficult or impossible to uniquely resolve their values (*33*). It is only because binding to the PRE is weakly cooperative that we were able to resolve this parameter.

In contrast to the small intrasite cooperativity term, the resolved intersite cooperativity parameter is large and negative, having a value of −3.3 kcal/mol. This free energy term translates to a 400-fold increase in overall binding affinity and thus a 20-fold increase in the per-site binding affinity (*32*). Further, it is qualitatively consistent with the same parameter resolved in the dimer binding model (−2.5 kcal/mol), although the results are slightly outside the 67% confidence intervals. If PR-B is competent to bind response elements as a monomer, this discrepancy might suggest that there are additional types of cooperativity not accounted for in our model (e.g., an intersite cooperative contribution to the triply ligated state.) Additional reduced-valency templates will be necessary to realistically examine this possibility. Shown in Figure 5c are the predicted binding isotherms when plotted in units of free PR-B monomer concentration. Unlike the large difference seen between plots in Figure 5a,b, the minimal change in plot 5a compared to 5c is partly due to the weak dimerization constant resulting in the PR-B monomer concentration to be nearly identical to the PR-B total protein concentration. Second, since the stoichiometry of monomer binding at each palindromic PRE is 2:1, the cooperative increase in affinity seen between binding at PRE_{1-} and PRE_2 appears only as the square root of the 20-fold per-site cooperativity term—about a 4.5-fold increase.

DISCUSSION

Insight into cooperative protein−DNA binding mechanisms requires resolution of the microscopic energetics of binding; macroscopic "apparent" binding affinities are of limited utility since they typically represent a composite of highly correlated interaction parameters. Quantitative DNAse footprint titration is one of the few techniques that is capable of accurately resolving these values. For this particular study, the symmetry relationships inherent in the identical PRE binding sites, and the independent determination of the PR-B dimerization constant were also critical and necessary factors in completing the analysis. The implications of the results on PR-B function are discussed below.

Interactions at Individual Response Elements: Intrinsic versus Apparent Binding Affinities. As seen in Figure 5a, a PR-B dimer (regardless of kinetic binding mechanism) has an *apparent* affinity toward a single PRE of approximately 12 nM. The receptor also shows evidence of intersite cooperativity when binding is analyzed on a promoter containing two PREs. These results are entirely consistent with previous semiquantitative analyses of PR−PRE interactions carried out under similar solution conditions (*8*, *12*). However, the quantitative analyses presented here reveal new and surprising information unobtainable from those earlier studies. Most striking is that the intrinsic affinity of a preformed PR-B solution dimer toward an individual PRE is not 12 nM, but rather 81 pM. Although this roughly 150-fold increase in affinity may seem unexpected in the context of nuclear receptor biochemistry, a picomolar affinity for a DNA binding protein under low salt concentration is not out of the ordinary. What the binding affinity of PR-B dimers might be under physiological conditions is difficult to estimate, since not only does the intrinsic binding affinity likely decrease as a function of increasing salt concentration (*34*), but the dimerization constant is also strongly salt dependent (*19*). Thus, if PR-B binds to response elements as a preformed solution dimer, then these two forces conspire to greatly weaken the apparent binding affinity as the salt concentration is increased. This may explain why biochemical studies of receptor−DNA interactions have historically been carried out under low salt (50−75 mM) conditions.

Perhaps even more surprising is the intrinsic affinity for a putative monomer binding pathway. The intrinsic affinity for a PR-B monomer toward an individual half-site is 39 nM (Table 2). This result suggests that it should be possible to directly measure binding of PR-B at an isolated half-site (even though the dogma states that this reaction is not kinetically allowed). Our own attempts to determine whether PR-B binds to an individual half-site have been equivocal: Footprint titration studies using a promoter template that contains only a single half-site demonstrate that the sequence becomes occupied in the nanomolar range exactly as predicted by our model, but half-site occupancy is also coupled to nonspecific binding in the surrounding flanking sequences, making quantitation and interpretation difficult (data not shown). Notwithstanding this result, only rigorous pre-steady-state kinetic analyses will definitely reveal whether

PR-B (or other steroid receptors) can interact with its response elements as a monomer or dimer, and this work is ongoing in our laboratory.

A second outcome of the monomer pathway analysis is that there is minimal intrasite cooperativity. That is, the binding of one PR-B monomer to a PRE half-site increases the affinity of binding a second monomer by only 5-fold (−0.9 kcal/mol), making the binding isotherm for binding to PRE_{1-} nearly Langmuir in shape. This result stands in sharp contrast to the highly cooperative binding transitions seen when deletion constructs of glucocorticoid receptor and progesterone receptor dimerize on their response elements (*11*, *25*, *26*, *35*). If PR-B monomers bind DNA, this difference in cooperative binding suggests that residues outside the canonical DBD constrain the ability of the full-length receptor to assemble on the DNA. The quantification and functional implications of this constraint are explored later in the Discussion.

It is difficult to compare the resolved energetics to that of other steroid receptors since, with the possible exception of the estrogen receptor (ER), no thermodynamic DNA binding studies have been carried out on any other intact nuclear receptor. Fluorescence anisotropy and surface plasmon resonance studies of estrogen receptor interactions with palindromic response elements resolved apparent dissociation constants in the low nanomolar range (*36*, *37*). However, since these studies did not explicitly take into account ER self-assembly energetics, it is not possible to make direct comparisons to the present data. Comparison is made more difficult since an important distinction between the estrogen receptor and progesterone receptor is that the two proteins likely have significantly different dimerization constants, with ER dimerization thought to occur in the nanomolar range, while PR-B dimerization occurs in the micromolar range (*19*). The implications of the weak PR-B dimerization constant are presented in Figure 6. Shown is the fractional population of PR-B dimer as determined by analytical ultracentrifugation (*19*), and the fractional population distributions of the various ligation states of the PRE_2 promoter as predicted by the dimer-binding pathway and monomer-binding pathway energetics. As expected, all intermediate ligation states are significantly depressed due to the large intersite cooperativity term. Moreover, it is evident that regardless of which model we use to analyze the data, promoter binding occurs under receptor concentrations in which the hormone-bound protein is entirely monomeric. This observation raises the question as to whether the traditional model that only preformed receptor dimers interact with response elements is correct. Although it is possible for a DNA-binding protein to be largely monomeric in solution yet still bind as a preformed dimer (*38*), the results presented here clearly warrant a more critical investigation of PR-B binding mechanisms.

Consequences of a Large Intersite Cooperative Free Energy. Regardless of whether PR-B binds individual response elements as a preformed dimer or a DNA-induced dimer, binding to multiple response elements is coupled to a large intersite cooperative free energy ranging from −2.5 to −3.3 kcal/mol. This energetic contribution translates to a 99- to 400-fold increase in overall binding affinity (approximately 10- to 20-fold increase on a per site basis) and is in good agreement with the original report of a 100-fold

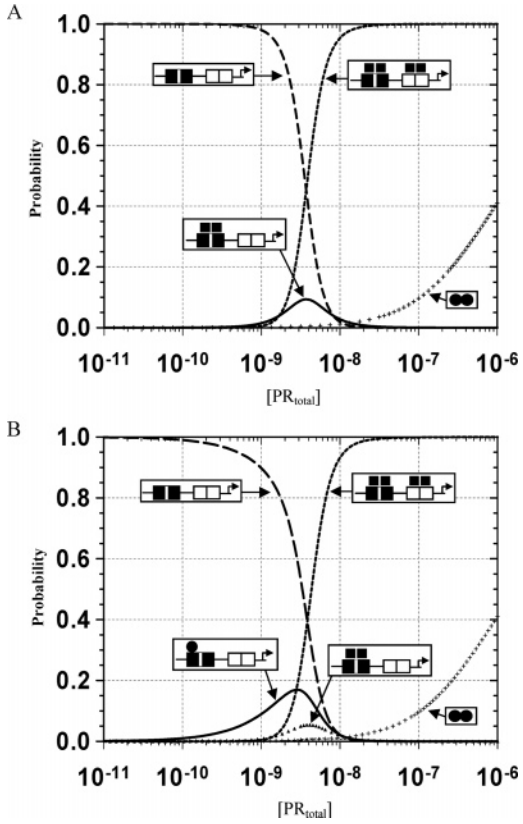

FIGURE 6: Predicted population distribution of each macroscopic PR-B:PRE_2 ligation state and proportion of PR-B solution dimers. (A) Population distribution of ligation states as predicted by the dimer-binding pathway energetics (Table 2). Unligated PRE_2 promoter (dashed line); singly ligated promoter (solid line); doubly ligated promoter (dotted line). Proportion of PR-B dimers is represented by "+" symbol. Schematic representations of each macroscopic ligation state are as described in Figure 2 and Table 1. (B) Population distribution of ligation states as predicted by the monomer-binding pathway energetics. Unligated PRE_2 promoter (dashed line); singly ligated promoter (solid line); doubly ligated promoter (triangles); fully ligated promoter (dotted line). Proportion of PR-B dimers is represented by "+" symbol. The triply ligated state never reaches more than 1% of the population and is thus not shown. Schematic representations of each macroscopic ligation state are as described in Figure 2 and Table 1.

increase in affinity as seen by O'Malley and co-workers (*12*). Intriguingly, the resolved cooperative free energies are nearly identical to those seen in the *c*I repressor-right operator system of bacteriophage λ (*39*, *40*). The large intersite cooperativity associated with *c*I repressor binding to the right operator ensures a stable but highly efficient molecular switch (*41*): Minor fluctuations in repressor levels do not cause a change in transcriptional response due to the enhanced stability of the repressor−DNA complex, but significant changes in repressor levels associated with various environmental insults cause a rapid and irreversible transition to the lytic phase. Presumably, the cooperative contributions to this system need to be large since only two proteins, *c*I repressor and *cro* repressor, regulate the switch from lysogeny to lysis. By contrast, in the eukaryotic environment PR-B is likely to be only one of roughly 50 proteins involved in transcriptional regulation of a single promoter (*42*, *43*). Further, these interactions appear to be highly unstable, kinetically driven processes. Thus, while many of the protein−protein and protein−DNA interactions are likely to be cooperative,

cooperativity at the level of PR-B:PRE interactions might be expected to be only moderate to not overwhelm efficient and responsive promoter function. The large degree of cooperativity seen in the PRE_2 system (and the strong PR-B mediated transcriptional response seen on this promoter) may thus be more a consequence of artificially creating multiple palindromic binding sites for PR-B and less a reflection of the properties of a natural PR-regulated promoter. This may further suggest that the role of cooperativity in higher eukaryotic systems serves a different role than for viruses such as bacteriophage λ. Exactly what that role might be remains speculative until we obtain an understanding of how the time-dependent microscopic configurations of PR binding (and associated coactivator interactions) are coupled to transcriptional activation.

The molecular mechanisms underlying intersite cooperative binding in nuclear receptors are unclear. Unlike the case of λ cI repressor, there is no evidence for a domain associated with cooperativity (*41*). Our own limited proteolysis and chemical cross-linking studies of the PR-B:PRE_2 complex show no indication of large-scale protein structural transitions or direct protein−protein interactions associated with cooperative assembly (data not shown). However, as discussed earlier, examination of the PRE_2 footprint (Figure 4a) shows hypersensitive bands coincident only with cooperative PR-B binding. It is thus likely that the molecular origins of intersite cooperativity are coupled to conformational changes in the DNA. Additionally, bending of the promoter complex may be associated with forming the proper architecture for recruitment of additional transcription factors, beyond allowing close contact of adjacent receptor dimers. If this is the case, the intrinsic interaction energetics between receptor dimers must be quite strong, since DNA bending would normally be expected to penalize cooperative interactions. Further analysis of the hypersensitive sites associated with intersite cooperativity and their role in PR-B binding mechanisms is currently under investigation.

Unfavorable Contributions to PR-B Binding at Individual PREs. This thermodynamic analysis of PR-B/DNA interactions demonstrates that receptor dimers, and potentially monomers, bind with unexpectedly high affinity. However, an analysis of the parameters in Table 2 reveals that binding to individual response elements is also accompanied by a large energetic penalty. This penalty is exemplified by comparing the free energy of forming a PR-B dimer from two monomers in solution ($\Delta G_{di} = -7.2$ kcal/mol) (*19*) versus forming the dimer from two monomers bound to a palindromic PRE ($\Delta G_{c1} = -0.9$ kcal/mol). By simple arithmetic, it is evident that dimerization on the PRE (i.e., DNA-induced dimerization) is associated with a +6.3 kcal/mol unfavorable contribution compared to solution dimerization. Importantly, since the free energy change associated with saturating a promoter is conserved regardless of the binding pathway, this unfavorable contribution can equally be interpreted as a penalty against a preformed dimer binding to a palindromic PRE: As seen in Table 2, a dimer binding to a PRE is associated with a −12.8 kcal/mol free energy change, while the energy change associated with adding two monomers to a PRE is −18.8 kcal/mol. Thus, dimer binding is energetically penalized relative to successive monomer binding by +6.0 kcal/mol. This penalty, termed a connection free energy ($\Delta G_{connect}$) by Jencks (*44*), must hold regardless of which kinetic pathway PR-B follows. Indeed, it can be visualized in the data as the weakly cooperative binding transition seen in the PRE_{1-} binding isotherm (Figure 3a).

Functional Consequences of an Allosteric or Structural Constraint. It is quite likely that the observed thermodynamic penalty reflects the cost of rearranging steroid receptor or DNA structure upon binding at PR-regulated promoters. As observed by biochemical and spectroscopic approaches, numerous studies have demonstrated that steroid receptor binding at response elements is accompanied by large-scale structural changes outside the canonical DNA binding domain (DBD) (*25*, *26*, *45*−*47*). These changes are often localized to unstructured (possibly natively unfolded) transcriptional activation domains and are thought to be coupled to recruitment of coactivating proteins. In light of the enormous energetic cost associated with binding, it is difficult to imagine that these structural changes are not dramatic and important, even if they can appear subtle by macroscopic measurements. As alluded to earlier, it is also likely that the penalty is associated with bending of the palindromic response element as seen in both promoter templates (see Figure 3a,b, small arrows). With the present data, it is not possible to dissect the energetic penalty into its protein and DNA-mediated contributions, although a procedure for doing so has been developed (*48*). If it is the case that this penalty is indeed associated with a functionally linked rearrangement of receptor structure, the present work represents the first step toward a physical understanding of interdomain communication in an intact nuclear receptor.

A second functional possibility is based on a thermodynamic argument rather than a structural one. Although steroid receptors can exist in solution as monomers and dimers, one would predict that the dimer species should dominate DNA binding simply because the rotational and translational entropic costs associated with saturating a palindromic PRE are paid only once (*49*). However, the unfavorable contribution to PR-B binding attenuates this inherent advantage to dimers and thus allows monomers to (putatively) compete with the dimers for interactions at response elements. As represented in Figure 6b, the energetic penalty to PR-B dimer binding results in the singly ligated promoter state to be significantly elevated over a broad concentration range compared to the doubly and triply ligated states. In the absence of the energetic penalty, the population of all intermediate ligation states would be minimal, causing PR-B binding at the PRE_2 promoter to result in a two-state switch, either fully saturating or desaturating the entire promoter. Given the complexity of eukaryotic promoter function, the functional utility of a two-state switch is unclear. It is worth hypothesizing that the unfavorable contribution to PR-B binding thus serves to enhance the role of monomer function via populating singly ligated intermediate states; this may be especially relevant if natural promoters contain multiple half-site response elements as is suggested by computer analysis. Clearly, more detailed analyses of steroid receptor−promoter interactions will be necessary to confirm the roles of monomers, dimers, and microstate configurations in transcriptional activation. In particular, thermodynamic studies of the A-isoform of PR will reveal whether it follows a similar or different trend as the B-isoform and whether the results might explain the unique transcriptional and functional properties of the two proteins.

ACKNOWLEDGMENT

We thank Dr. Dean Edwards and Dr. Kathryn Horwitz for constructs. We thank Dr. Carlos Catalano and Dr. N. Karl Maluf for helpful discussions.

REFERENCES

1. Tsai, M. J., and O'Malley, B. W. (1994) Molecular mechanisms of action of steroid/thyroid receptor superfamily members, *Annu. Rev. Biochem. 63*, 451−486.
2. Takimoto, G. S., Tung, L., Abdel-Hafiz, H., Abel, M. G., Sartorius, C. A., Richer, J. K., Jacobsen, B. M., Bain, D. L., and Horwitz, K. B. (2003) Functional properties of the N-terminal region of progesterone receptors and their mechanistic relationship to structure, *Steroid Biochem. Mol. Biol. 85*, 209−219.
3. Sartorius, C. A., Melville, M. Y., Hovland, A. R., Tung, L., Takimoto, G. S., and Horwitz, K. B. (1994) A third transactivation function (AF3) of human progesterone receptors located in the unique N-terminal segement of the B-isoform, *Mol. Endocrinol. 8*, 1347−1360.
4. Richer, J. K., Jacobsen, B. M., Manning, N. G., Abel, M. G., Wolf, D. M., and Horwitz, K. B. (2002) Differential gene regulation by the two progesterone receptor isoforms in human breast cancer cells, *J. Biol. Chem. 277*, 5209−5218.
5. Hurd, C., Nag, K., Khattree, N., Alban, P., Dinda, S., and Moudgil, V. K. (1999) Agonist and antagonist-induced qualitative and quantitative alterations of progesterone receptor from breast cancer cells, *Mol. Cell. Biochem. 199*, 49−56.
6. Conneely, O. M., Mulac-Jericevic, B., Lydon, J. P., and DeMayo, F. J. (2001) Reproductive functions of the progesterone receptor isoforms: lessons from knock-out mice, *Mol. Cell Endocrinol. 179*, 97−103.
7. Hopp, T. A., Weiss, H. L., Hilsenbeck, S. G., Cui, Y., Alfred, D. C., Horwitz, K. B., and Fuqua, S. (2004) Breast cancer patients with progesterone receptor PR-A-rich tumors have poorer disease-free survival rates, *Clin. Cancer Res. 15*, 2751−2760.
8. Onate, S. A., Prendergast, P., Wagner, J. P., Nissen, M., Reeves, R., Pettijohn, D. E., and Edwards, D. P. (1994) The DNA-bending protein HMG-1 enhances progesterone receptor binding to its target DNA sequence, *Mol. Cell. Biol. 14*, 3376−3391.
9. Rodriguez, R., Weigel, N. L., O'Malley, B., and Schrader, W. T. (1990) Dimerization of the chicken progesterone receptor in vitro can occur in the absence of hormone and DNA, *Mol. Endocrinol. 4*, 1782−1790.
10. DeMarzo, A. M., Beck, C. A., Onate, S. A., and Edwards, D. P. (1991) Dimerization of mammalian progesterone receptors occurs in the absence of DNA and is related to the release of the 90-kDa heat shock protein, *Proc. Natl. Acad. Sci., U.S.A. 88*, 72−76.
11. Tsai, S. Y., Carlstedt-Duke, J., Weigel, N. L., Dahlman, K., Gustafsson, J.-A., Tsai, M.-J., and O'Malley, B. W. (1988) Molecular interactions of steroid hormone receptor with its enhancer element: evidence for receptor dimer formation, *Cell 55*, 361−369.
12. Tsai, S. Y., Tsai, M.-J., and O'Malley, B. W. (1989) Cooperative binding of steroid hormone receptors contributes to transcriptional synergism at target enhancer elements, *Cell 57*, 443−448.
13. Truss, M., and Beato, M. (1993) Steroid hormone receptors: interaction with deoxyribonucleic acid and transcription factors, *Endocr. Rev. 14*, 459−479.
14. Bailly, A., Rauch, C., Cato, A. C. B., and Milgrom, E. (1991) In two genes, synergism of steroid hormone action is not mediated by cooperative binding of receptors to adjacent sites, *Mol. Cell. Endocrinol. 82*, 313−323.
15. Cato, A., Henderson, D., and Ponta, H. (1987) The hormone response element of the mouse mammary tumor virus DNA mediates the progestin and androgen induction of transcription in the proviral long terminal repeat region, *EMBO J. 6*, 363−368.
16. Chalepakis, G., Arnemann, J., Slater, E., Bruller, H.-J., Gross, B., and Beato, M. (1988) Differential gene activation by glucocorticoids and progestins through the hormone regulatory element of mouse mammary tumor virus, *Cell 53*, 371−382.
17. Perlmann, T., Eriksson, P., and Wrange, O. (1990) Quantitative analysis of the glucocorticoid receptor-DNA interaction at the mouse mammary tumor virus glucocorticoid response element, *J. Biol. Chem. 265*, 17222−17229.
18. Christensen, K., Estes, P. A., Onate, S. A., Beck, C. A., DeMarzo, A., Altmann, M., Lieberman, B. A., St. John, J., Nordeen, S. K., and Edwards, D. P. (1991) Characterization and functional properties of the A and B forms of human progesterone receptors synthesized in a baculovirus system, *Mol. Endocrinol. 5*, 1755−1770.
19. Heneghan, A. F., Berton, N., Miura, M. T., and Bain, D. L. (2005) Self-association energetics of an intact, full-length nuclear receptor: the B-isoform of human progesterone receptor dimerizes in the micromolar range, *Biochemistry 44*, 9528−9537.
20. Jantzen, H. M., Strahle, U., Gloss, B., Stewart, F., Schmid, W., Boshart, M., Miksicek, R., and Schutz, G. (1987) Cooperativity of glucocorticoid response elements located far upstream of the tyrosine aminotransferase gene, *Cell 49*, 29−38.
21. Eriksson, P., and Wrange, O. (1990) Protein−protein contacts in the glucocorticoid receptor homodimer influences its DNA binding properties, *J. Biol. Chem. 265*, 3535−3542.
22. Sambrook, J., Fritsch, E. F., and Maniatas, T. (1989) *Molecular Cloning A Laboratory Manual*, Cold Spring Harbor Laboratory Press, Woodbury, NY.
23. Brenowitz, M., Senear, D. F., Shea, M. A., and Ackers, G. K. (1986) Quantitative DNase footprint titration: a method for studying protein-DNA interactions, *Methods Enzymol. 130*, 132−181.
24. Brenowitz, M., Senear, D. F., Shea, M. A., and Ackers, G. K. (1986) Footprint titrations yield valid thermodynamic isotherms, *Proc. Natl. Acad. Sci. U.S.A. 83*, 8462−8466.
25. Bain, D. L., Franden, M. A., McManaman, J. L., Takimoto, G. S., and Horwitz, K. B. (2000) The N-terminal region of the human progesterone A-receptor: structural analysis and the influence of the DNA binding domain, *J. Biol. Chem. 275*, 7313−7320.
26. Bain, D. L., Franden, M. A., McManaman, J. L., Takimoto, G. S., and Horwitz, K. B. (2001) The N-terminal region of human progesterone B-receptors: biophysical and biochemical comparison to A-receptors, *J. Biol. Chem. 276*, 23825−23831.
27. Cohen-Solal, K., Bailly, A., Rauch, C., Quesne, M., and Milgrom, E. (1993) Specific binding of progesterone receptor to progesterone-responsive elements does not require prior dimerization, *Eur. J. Biochem. 214*, 189−195.
28. Ackers, G. K., Johnson, A. D., and Shea, M. A. (1982) Quantitative model for gene regulation by lambda phage repressor, *Proc. Natl. Acad. Sci. U.S.A. 79*, 1129−1133.
29. Hill, T. L. (1960) *An Introduction to Statistical Thermodynamics*, Dover Publications, New York.
30. Dabrowiak, J. C., and Goodisman, J. (1989) in *Chemistry and Physics of DNA-Ligand Interactions* (Kallenback, N. R., Ed.), Adenine Press, Schenectady, NY.
31. Petz, L. N., Nardulli, A. M., Kim, J., Horwitz, K. B., Freedman, L. P., and Shapiro, D. J. (1997) DNA bending is induced by binding of the glucocorticoid receptor DNA binding domain and progesterone receptors to their response elements, *J. Steroid Biochem. 60*, 31−41.
32. Ackers, G. K., Shea, M. A., and Smith, F. R. (1983) Free energy coupling within macromolecules. The chemical work of ligand binding at the individual sites in cooperative systems, *J. Mol. Biol. 170*, 223−242.
33. Senear, D. F., Brenowitz, M., Shea, M. A., and Ackers, G. K. (1986) Energetics of cooperative protein-DNA interactions: comparison between quantitative deoxyribonuclease footprint titration and filter binding, *Biochemistry 25*, 7344−7354.
34. Record, M. T., Anderson, C. F., and Lohman, T. M. (1978) Thermodynamic analysis of ion effects on the binding and conformational equilibria of proteins and nucleic acids: the roles of ion association or release, screening, and ion effects on water activity, *Quant. Rev. Biophys. 11*, 103−178.
35. Lundback, T., Cairns, C., Gustafsson, J. A., Carlstedt-Duke, J., and Hard, T. (1993) Thermodynamics of the glucocorticoid receptor DNA interaction- binding of wild-type GR-DBD to different response elements, *Biochemistry 32*, 5074−5082.
36. Cheskis, B. J., Karathanasis, S., and Lyttle, C. R. (1997) Estrogen receptor ligands modulate its interaction with DNA, *J. Biol. Chem. 272*, 11384−11391.
37. Boyer, M., Poujol, N., Margaret, E., and Royer, C. A. (2000) Quantitative characterization of the interaction between purified human estrogen receptor and DNA using fluoresence anisotropy, *Nucleic Acids Res. 28*, 2494−2502.
38. Streaker, E. D., and Beckett, D. (2003) Coupling of protein asembly and DNA binding: biotin repressor dimerization precedes biotin operator binding, *J. Mol. Biol. 325*, 937−948.

39. Senear, D. F., and Ackers, G. K. (1990) Proton-linked contributions to site-specific interactions of lambda cI repressor and "OR", *Biochemistry 28*, 6568−6577.
40. Senear, D. F., and Brenowitz, M. (1991) Determination of binding constants for cooperative site-specific protein-DNA interactions using the gel mobility-shift assay, *J. Biol. Chem. 266*, 13661−13671.
41. Ptashne, M. (1986) *A Genetic Switch: Gene Control and Phage Lambda*, Cell Press, Cambridge, MA, Blackwell Scientific Publications, Palo Alto, CA.
42. Metivier, R., Penot, G., Hubner, M. R., Reid, G., Brand, H., Kos, M., and Gannon, F. (2003) Estrogen receptor-alpha directs ordered, cyclical, and combinatorial recruitment of cofactors on a natural target promoter, *Cell 115*, 751−763.
43. Nagaich, A. K., Walker, D. A., Wolford, R., and Hager, G. L. (2004) Rapid periodic binding and displacement of the glucocorticoid receptor during chromatin remodeling, *Mol. Cell 14*, 163−174.
44. Jencks, W. P. (1981) On the attribution and additivity of binding energies *Proc. Natl. Acad. Sci., U.S.A. 78*, 4046−4050.
45. Kumar, R., and Thompson, E. B. (2003) Transactivation functions of the N-terminal domains of nuclear hormone receptors: protein folding and coactivator interactions, *Mol. Endocrinol. 17*, 1−10.
46. Warnmark, A., Treuter, E., Wright, A. P. H., and Gustafsson, J.-A. (2003) Activation functions 1 and 2 of nuclear receptors: molecular strategies for transcriptional activation, *Mol. Endocrinol. 17*, 1901−1909.
47. Brodie, J., and McEwan, I. J. (2005) Intra-domain communication between N-terminal and DNA-binding domains of the androgen receptor: modulation of androgen response element DNA binding, *J. Mol. Endocrinol. 34*, 603−615.
48. Rusinova, E., Ross, J. B., Laue, T. M., Sowers, L. C., and Senear, D. F. (1997) Linkage between operator binding and dimer to octamer self-assembly of bacteriophage lambda cI repressor, *Biochemistry 42*, 2994−3003.
49. Creighton, T. E. (1983) *Proteins, Structure and Molecular Principles*, W. H. Freeman and Company, New York.

BI052046G